Theoretical Study on the Mechanism and Diastereoselectivity of $NaBH_4$ Reduction

Yasumitsu Suzuki, Daisuke Kaneno, and Shuji Tomoda*

Department of Life Science, Graduate School of Arts and Sciences, The University of Tokyo, Komaba, Meguro-ku, Tokyo 153-8902, Japan

Received: November 12, 2008; Revised Manuscript Received: December 26, 2008

As the first step to understand the reaction mechanism and diastereoselectivity of sodium borohydride reduction of ketones, ab initio Car−Parrinello molecular dynamics simulation has been performed on a solution of $NaBH_4$ in liquid methanol. According to pointwise thermodynamic integration involving constrained molecular dynamics simulations, it was strongly suggested that Na^+ and BH_4^- are associated in the solvent forming contact ion pairs. Thus we propose a new transition state structure model that contains complexation of the carbonyl oxygen with sodium cation. Predicted diastereoselectivity of the reduction of some substituted cyclohexanones applying this novel transition state model is in good agreement with experimental data, showing its validity and effectiveness to investigate the diastereoselectivity of $NaBH_4$ reduction of other ketones.

Introduction

Since sodium borohydride was discovered by Schlesinger and Brown and their co-workers in 1943,[1] it has been widely used as a reducing agent in organic synthesis and other various fields. One of the advantages to use $NaBH_4$ for reduction is its characteristic chemoselectvity that arises from its mild reducing ability. Furthermore, $NaBH_4$ exhibits a high degree of π-facial diastereoselectivity, which can produce, for example, one diastereomeric alcohol predominantly in the reduction of prochiral ketone. The origin of this diastereoselectivity has been the very significant subject of many research papers for half a century.[2] In the case of lithium aluminum hydride reduction, which also shows a high π-facial diastereoselectivity, there is an established theory that explains the mechanism of the reaction to predict correct diastereoselectivity.[2c,3−12] On the other hand, in the case of $NaBH_4$ reduction, there is still a lack of reliable theory that can describe the reaction mechanism. Although some theories based on a simplified transition state model have been reported by Houk et al.,[13] these are only able to make qualitative analysis and in some cases lead to a wrong prediction.[2c,14] Basically, quantitative prediction of diastereoselection must be achieved by the calculation based on the transition state theory that uses a reliable transition state structure gained by an ab initio theory, which has not been established so far. In 1977, Wigfield discussed several transition state geometry models of $NaBH_4$ reduction which do not contain the role of the sodium cation (Scheme 1).[15−17]To this end, many researchers assumed that the transition state of $NaBH_4$ reduction does not contain sodium cation in their study,[18−22] and some researchers used the transition state model that is similar to the one proposed by Wigfield to discuss the origin of π-facial diastereoselectivity.[22] On the other hand, however, there have been a number of reports against Wigfield's proposal which insist that sodium cation plays some role on the reaction mechanism of $NaBH_4$ reduction. Glass et al.[23] showed that the diastereomeric product ratio of $NaBH_4$ reduction was dramatically changed when sequestration of the sodium cation by adding crown ether was done, and Yadav et al.[14] showed that the consideration of the cation complexation

SCHEME 1: Transition State Geometries Discussed by Wigfield et al.

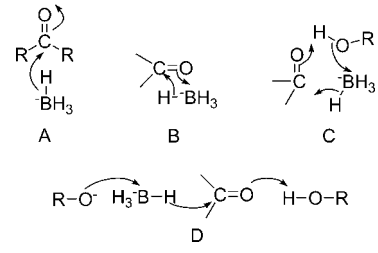

to the carbonyl oxygen is needed to explain π-facial diastereoselectivity of $NaBH_4$ reduction with 2-*ax*- and 2-*eq*-substituted cyclohexanones. But after all, comprehensive theoretical studies with high level ab initio calculation to clarify the mechanism of $NaBH_4$ reduction have not been conducted so far, which is necessary for detailed investigation about the origin of π-facial diastereoselectivity and the correct prediction of diastereomeric product ratios.

In this work, first, the nature of the solute species of $NaBH_4$ present in methanol solvent was investigated by ab initio Car−Parrinello molecular dynamics (CPMD)[24,25] simulations. Studies on the structural and dynamical property of solutes with CPMD simulations have been reported in many papers recently, and it is well-known that the method provides good results which cannot be gained by classical molecular dynamics simulations in a wide variety of aspects.[26] To assess the relative stability of various states of $NaBH_4$, we calculated the free energy profiles for the dissociation process in methanol solvent using the pointwise thermodynamic integration (PTI)[27] technique. The data obtained show that $NaBH_4$ is associated in methanol solvent forming contact ion pairs. The result suggests that also in the transition state of the reduction of ketones, Na^+ and BH_4^- may be associated. Then we have successfully located such a transition state structure of $NaBH_4$ reduction using high-level DFT calculations and performed IRC calculation to confirm whether or not this structure is valid. Finally, by using this novel transition state structure, the diastereomeric product ratio of $NaBH_4$ reduction with some substituted cyclohexanones, which show different experimental π-facial diastereoselectivity,

* Corresponding author. Phone: +81-3-5454-6575. Fax: +81-3-5454-6998. E-mail: tomoda@selen.c.u-tokyo.ac.jp.

10.1021/jp809966u CCC: $40.75
Published on Web 02/16/2009

TABLE 1: Selected Structural Data of the $CH_3OH\cdots NaBH_4$ System[a]

	BLYP/PW[b]	B3LYP/G[c]	MP2/G[c]
$r_{O\cdots Na}$	2.323	2.271	2.339
r_{O-H}	0.974	0.959	0.958
r_{O-C}	1.483	1.442	1.441
$r_{Na\cdots B}$	2.376	2.325	2.362
$\langle r_{B-H}\rangle$[d]	1.233	1.230	1.227
$\theta_{Na\cdots O-H}$	138.6	137.7	139.2
$\theta_{Na\cdots O-C}$	113.9	112.9	112.3
$\theta_{O\cdots Na-B}$	125.1	124.2	113.5
$E_{binding}(Na\cdots BH_4)$ (kcal mol^{-1})	−96.5	−90.2	−96.0
$E_{binding}(NaBH_4\cdots methanol)$ (kcal mol^{-1})	−13.5	−14.1	−14.7

[a] Distances r in Å and angles θ in deg. [b] Plane waves expansion. [c] Gaussian basis sets 6-311++G(3df,3pd). [d] Average value.

was calculated. Some discussion about these results and further perspectives are also given.

Computational Details

Car−Parrinello Molecular Dynamics Simulations. Car−Parrinello molecular dynamics simulations have been performed with the CPMD program[28] in a cubic box of 10.50 Å side, with periodic boundary conditions and 15 methanol molecules and one $NaBH_4$, which corresponds to the density of methanol, 0.79. We have adopted Martins−Troullier (MT)[29] pseudopotentials along with the Kleinman−Bylander[30] decomposition for the C and O atoms, whereas a Von Barth−Car[31] pseudopotential has been adopted for the H atoms; it is known that this choice has been shown to give good results for pure liquid methanol.[32] Norm-conserving pseudopotentials of the Goedecker, Teter, Hutter (GTH) type[33] have been used for the B and Na atoms. The same choice for the ions was made by Faralli et al.[34] Kohn−Sham orbitals were expanded in plane waves at the Γ-point up to a kinetic energy cutoff of 70 Ry, following previous studies on liquid methanol[32] and on ions in methanol.[34−37] The BLYP[38,39] exchange-correlation functional have been used for density functional calculations. To validate this computational strategy, the structure and some of the electronic properties of the CH_3OH complex with $NaBH_4$ have been calculated by our approach and compared with the result of DFT and MP2 optimize calculations by using the localized Gaussian basis set, 6-311++G(3df,3pd), implemented in the Gaussian 03 programs.[40] The data obtained are summarized in Table 1, showing that our computational method satisfactorily reproduces the structural parameters of the CH_3OH complex with $NaBH_4$ and the binding energy between Na^+(coordinating methanol) and BH_4^- as well as $NaBH_4$ and methanol.

The initial configuration of simulation was set so that $NaBH_4$ is located on the center of the supercell and methanol molecules form a simple cubic lattice around $NaBH_4$, where each structure of $NaBH_4$ and methanol was optimized by DFT calculations with Gaussian 03 beforehand. Then CPMD simulations at high temperature (1000 K) by velocity scaling were performed with a time step of 4 au (∼0.1 fs) for 1 ps, in which coordinates of $NaBH_4$ were fixed. After that, unconstrained CPMD simulations were performed in the NVT ensemble with a Nosé-Hoover chain thermostat set to 300 K over 5 ps for the purpose of thermal equilibration. Finally, CPMD simulations for the sampling were performed over 5 ps in the NVT ensemble with a Nosé-Hoover chain thermostat set to 300 K, a fictitious electronic mass of 400 au, and a time step of 4 au (∼0.1 fs).

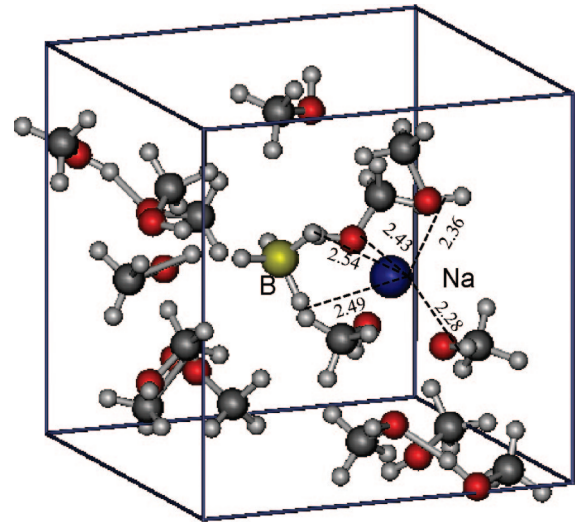

Figure 1. Snapshot of the solvation shell for $NaBH_4$.

To evaluate the change in the Helmholtz free energy by pointwise thermodynamic integration (PTI),[27] constrained CPMD simulations were performed along a predefined reaction coordinate (see the Results and Discussion section below). We chose one $Na\cdots B$ distance r as the reaction coordinate and increased its value successively in steps of 0.20 Å. At each point, the system was propagated until the mean constrained force, $\langle f\rangle$, was sufficiently converged (usually within 2 ps). These simulations were performed also in the NVT ensemble with a Nosé-Hoover chain thermostat set to 300 K.

Optimization of Transition State Structure. All geometries of reactants, products, and transition state structures for the reaction of $NaBH_4$ with acetone and several substituted cyclohexanones were optimized by using DFT calculations with B3LYP hybrid functional[39,41] and 6-31+G(d) basis set, adopting the Gaussian 03 programs.[40] The energies of each structures were calculated by the MP2 method with the 6-31+G(d) basis set. Stationary points were fully optimized and characterized by vibrational frequency calculations that also provided zero-point vibrational energies (ZPE). One negative imaginary frequency was found for each transition state and the direction of hydride vibration in the transition state is from atom B toward the carbonyl carbon. Intrinsic reaction coordinate (IRC) calculations for each transition state structure were also performed.

Results and Discussion

$NaBH_4$ in Liquid Methanol. We first report the results of Car−Parrinello molecular dynamics simulations about a solution of $NaBH_4$ in liquid methanol. The snapshot of the solvation shell of the $NaBH_4$ during the simulation performed at 300 K over 5 ps is shown in Figure 1. One can see from Figure 1 that sodium cation Na^+ is coordinated by three methanol oxygen atoms, and Na^+ and borohydride BH_4^- form a contact ion pair.

The most remarkable phenomenon of the simulation is that Na^+ and BH_4^- are never separated spontaneously throughout the run. The nonbonded $Na\cdots B$ distance along the simulation run is reported in Figure 2, which shows that the distance between Na^+ and BH_4^- fluctuated little around some certain value and never exceeded 3.3 Å. The time average of the distance is 2.74 Å. This result strongly suggests that $NaBH_4$ exists in the form of contact ion pairs in methanol solvents. The time variation of the coordination number of Na^+ by methanol oxygen during the simulation is reported in Figure 3. A molecule is defined to coordinate to Na^+ if the distance of

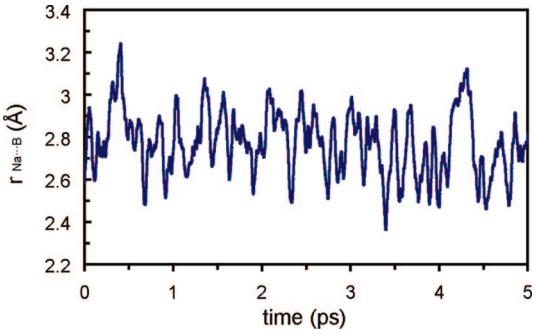

Figure 2. Na···B distance along the simulation run.

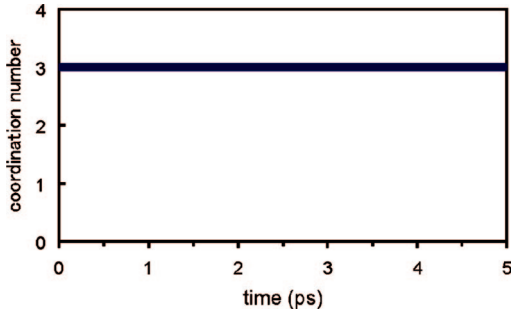

Figure 3. The instantaneous coordination number of Na^+ by methanol oxygen during the simulation run.

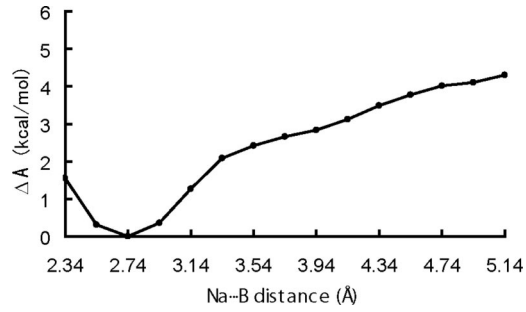

Figure 4. Change in free energy, ΔA, for the dissociation process of $NaBH_4$ in liquid methanol.

its oxygen atom from Na^+ is smaller than 3.79 Å, which is the sum of the van der Waals radii of sodium and oxygen. From Figure 3, it can be seen that three methanol molecules always coordinate Na^+ in the whole simulation time. If two hydrogens of BH_4^- are considered to coordinate Na^+, which looks so throughout the run, the total coordination number of Na^+ is counted as 5, which is in agreement with the previous theoretical study done by Faralli et al.[34] This also supports the validity of the present simulation.

To obtain further information about the relative stability of this form of contact ion pairs of $NaBH_4$, we performed constrained MD simulations along a predefined reaction coordinate connecting the form of contact ion pairs and the dissociated form and evaluated the change in the Helmholtz free energy by pointwise thermodynamic integration (PTI)[27] of the mean constraint force $\langle f \rangle$ via

$$\Delta A_{a\to b} = -\int_a^b \langle f(r) \rangle \, dr$$

We chose one Na···B distance r as the reaction coordinate and increased its value successively from 2.34 Å in steps of 0.20 Å. The resulting free energy profile for the dissociation process is shown in Figure 4. This result shows that there is only one minimum, corresponding to a contact ion pair, where the Na···B distance is ca. 2.7 Å and the coordination number of Na^+ by methanol oxygen is three, similar to the structure that was seen from the previous sampling run (its snapshot is depicted in Figure 1). More methanol molecules are able to come closer to Na^+ upon dissociation and finally five methnol molecules coordinate Na^+ when BH_4^- is sufficiently separated from Na^+, in agreement with Faralli's study.[34] Snapshots showing the coordination shell of $NaBH_4$ at different Na···B distances are depicted in Figure 5. These results about the free energy profile for the dissociation process of $NaBH_4$ are very similar to the previous study on that of $LiAlH_4$.[11] As can be seen from Figures 4 and 5, solvated ion pairs, in which $NaBH_4$ are separated by a methanol molecule, are not stable local minima like the dissociation process of $LiAlH_4$. Further, the free energy barrier to dissociation of of $NaBH_4$, ca. 5 kcal/mol, is somewhat larger than that of $LiAlH_4$, ca. 4 kcal/mol. This implies that Na^+ and BH_4^- are more strongly associated in solvents than Li^+ and AlH_4^-. It should be noted here that these results might underestimate the stabilizing effect of the separated ions a little because the cell size used in this study is somewhat small and it is shown by Hummer et al.[42] that the solvation free energy might be evaluated slightly lower in such a case. And our choice of the pseudopotentials and the performance of DFT should also be considered carefully again, though it is demonstrated in the Computational Details section that our method satisfactorily reproduces the structural parameters and the binding energy obtained from MP2 calculation adopted in Gaussian 03 programs. Even after taking them all into account, it can now state that Na^+ and BH_4^- may be associated in the transition state of reduction of ketone since in the case of $LiAlH_4$ reduction there are some established theories that state that Li^+ and AlH_4^- are associated in the transition state.[6,9,11]

$NaBH_4$ Reduction of Acetone. Considering the above results, it is natural to assume that Na^+ is associated with borohydride in the entire process of $NaBH_4$ reduction despite Wigfield's proposal.[16,17] So we searched for the transition state structure that includes Na^+ associating with BH_4^- elaborately and finally succeeded in locating such a transition state structure using DFT optimization (B3LYP/6-31+G(d)). Figure 6 shows this transition state structure in the case of the reduction of acetone. One can recognize from Figure 6 that this transition state structure is the cyclic form, which is similar to that of $LiAlH_4$ reduction, and has product-like geometries which are not similar to those of $LiAlH_4$ reduction; the forming C···H bond length of the transition state structure of $NaBH_4$ reduction is 1.13 Å, which is almost the same size as the bond length of the product alcohol, whereas the transition state structure of $LiAlH_4$ reduction has a reactant-like geometry, in which the forming C···H bond length is much longer than the bond length of the product.[9] In this respect, our new theory coincides with Wigfield's proposal, which also states that the transition state of $NaBH_4$ reduction is product-like.[17]

The result of normal mode vibration analysis about this transition state shows a vibration corresponding to a stretching vibration of the forming C···H bond. A calculation of intrinsic reaction coordinate (IRC) was performed with this transition state and the structures corresponding to the reactant, which is the complex of $NaBH_4$ and acetone, and the product are successfully located along both sides of IRC (Figures 7 and 8). The product structure (Figure 8) is the complex of the sodium salt of the corresponding alcohol, isopropanol, and BH_3. Thus, it can be said that the present transition state structure correctly illustrates the reaction of $NaBH_4$ reduction. It is estimated from Figure 7 that the reaction proceeds via initial complex formation

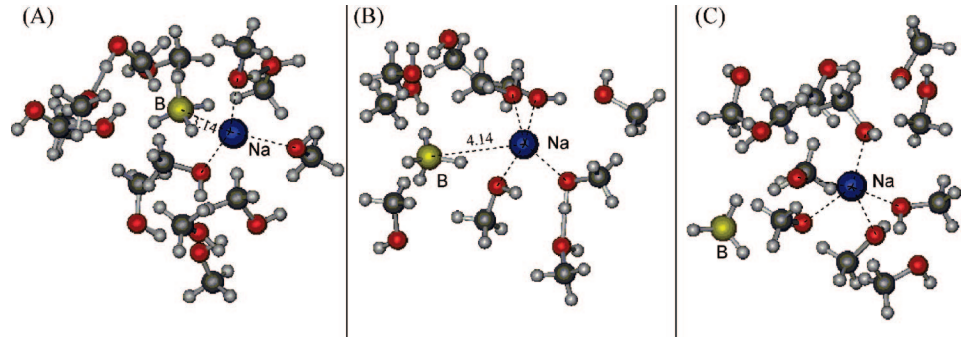

Figure 5. Snapshots of configurations of solvated $NaBH_4$: (A) Na···B distance is 3.14 Å; (B) Na···B distance is 4.14 Å; and (C) Na···B distance is 5.14 Å.

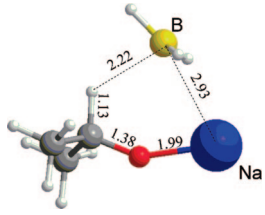

Figure 6. Transition state structure of $NaBH_4$ reduction of acetone (B3LYP/6-31+G(d)).

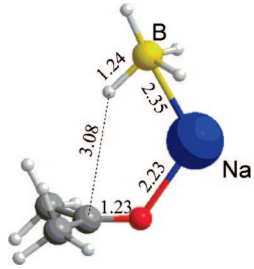

Figure 7. Reactant (complex of $NaBH_4$ and acetone) structure of $NaBH_4$ reduction of acetone (B3LYP/6-31+G(d)).

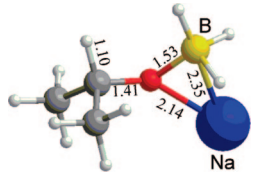

Figure 8. Product structure of $NaBH_4$ reduction of acetone (B3LYP/6-31+G(d)).

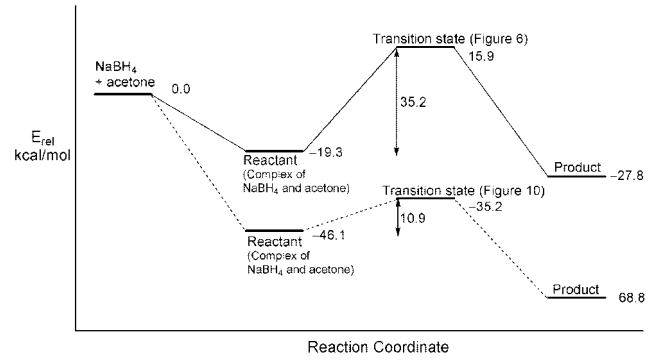

Figure 9. Energy diagram for the reaction coordinate of $NaBH_4$ reduction of acetone: (solid line) gas phase and (dashed line) considering three solvent molecules explicitly.

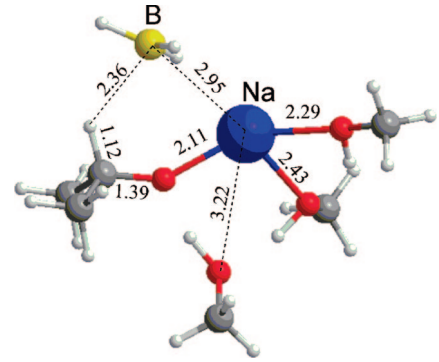

Figure 10. Transition state structure of $NaBH_4$ reduction of acetone with three methanol molecules coordinating Na^+ (B3LYP/6-31+G(d)).

of $NaBH_4$ and acetone, followed by nucleophilic attack of the sodium borohydride, which is like the reaction mechanism of $LiAlH_4$.

The energy diagram obtained for the reaction coordinate of $NaBH_4$ reduction of acetone is depicted in Figure 9. The calculated ZPE corrected activation energy of $NaBH_4$ reduction of acetone in the gas phase is 35.2 kcal/mol. This value is larger than that of $LiAlH_4$ reduction, which has a calculated value of 11.7 kcal/mol[43] in the bidentate transition state structure and 12.2 kcal/mol[43] in the tridentate transition state structure, coinciding with the experimental fact that the reducing power of $NaBH_4$ is milder than that of $LiAlH_4$ and also with Hammond postulate,[44] in the light of having a large activation energy when transition state structure is product-like. However, one can notice at this point that this activation energy (35.2 kcal/mol) is somewhat too high, so the reaction seems unlikely to occur. But, in the above calculation, we do not count solvent molecules (methanol in this study) upon the geometry of the transition state structure. In 1977 Wigfield et al. showed that the protic solvents do play a crucial catalytic role on the kinetics of $NaBH_4$ reduction and the transition state structure must involve the participation of protic solvent,[16,17] and in 1982 Eisenstein et al. showed that including solvent molecules in the calculation decreases the activation energy of $NaBH_4$ reduction.[19] Furthermore, the result of CPMD simulation in this study showed that three methanols almost always coordinate the sodium cation and form a stable cage in the solution, also strongly suggesting that solvent molecules must be included in the transition state structure. So we included three methanols in the transition state structure of $NaBH_4$ reduction with acetone in some appropriate way to stabilize the system, and again optimized using the DFT method (B3LYP/6-31+G(d)). As a result, we successfully obtained the transition state structure that contained three methanol molecules as depicted in Figure 10. As shown in Figure 10, three methanol molecules are arranged making hydrogen bonding to stabilize the system, and one methanol separated from the sodium cation slightly so that the total

TABLE 2: Experimental and Calculated Diastereomeric Product Ratios of 1 and 2

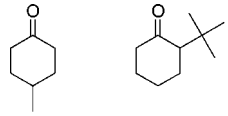

1 **2**

	ax-attack:eq-attack product ratios	
ketone	exptl ratio[46,47]	calcd ratio[a]
1	86:14[b]	80.9:19.1
2	50:50[c]	41.0:59.0
	43:57[d]	

[a] Ratios of transition states were calculated assuming Boltzmann distribution at 25 °C. See the text for details. [b] Reaction was performed at 25 °C. [c] Reaction was performed at 21 °C. [d] Reaction was performed at 82 °C.

coordination number of Na^+ is 5 as ever. Normal mode vibration analysis and IRC calculations were also done, and the results of IRC calculations are also summarized in Figure 9. It shows that the activation energy is only 10.9 kcal/mol, which is dramatically decreased from 35.2 kcal/mol (the value of the gas phase calculation), making the reaction much easier to occur. This enormous reduction of the activation energy might be the result of reduced electrophilicity of Na^+ caused by coordination of solvent molecules which may enhance the nucleophilicity of BH_4^-, significantly. From Figure 6, one can notice indeed that BH_4^- must be separated from Na^+ slightly and move to the position near the carbonyl carbon in the transition state (the distance between Na^+ and BH_4^- was elongated from 2.35 Å to 2.93 Å). The activation induced by this separation of $NaBH_4$ is small when the electrophilicity of Na^+ is reduced. Thus, the addition of solvent molecules can reduce the activation energy. Although three explicit solvent molecules may not represent the whole stabilizing effect of the higher solvation shells,[45] it satisfactorily reproduces the experimental value of the activation enthalpy (around 6−12 kcal mol^{-1}).[46] Now the catalytic effect of protic solvent is also recognized in the framework of our newly proposed transition state structure model, where the sodium cation plays a key role. All these results mentioned above strongly support the validity of our novel transition state structure, so subsequently we will discuss π-facial diastereoselectivity in the $NaBH_4$ reduction of some substituted cyclohexanones using this transition state structure.

π-Facial Diastereoselectivity in the $NaBH_4$ Reduction of Substituted Cyclohexanones. We now describe the results of the calculated diastereomeric product ratio in the $NaBH_4$ reduction using our newly proposed transition state structure. There have been so many reports in which the diastereomeric product ratios in $NaBH_4$ reduction of various ketones are investigated experimentally.[46,47] In the present study, to verify our theory we deal with two substituted cyclohexanones, which show remarkably different experimental diastereoselectivity as a good example. They are, 4-methylcyclohexanone (**1**), which shows a preference of axial attack of hydride, and 2-*tert*-butylcyclohexanone (**2**), which shows diastereoselectivity almost eliminated. Their diastereomeric product ratios (axial vs equatorial attack of hydride) in experiment[46,47] are summarized in Table 2.

For each cyclohexanone derivative, transition state structures in $NaBH_4$ reduction were fully optimized for both sides of the attack at the MP2/6-31+G(d)//B3LYP/6-31+G(d) level and confirmed by normal mode vibration analysis. We found that the transition state structure in which the substituent is in the axial position is energetically very unstable and their process ratio is nearly null, so we omitted those structures and considered only the structure in which the substituent is in the equatorial position in this study. Figures 11 and 12 show the calculated transition state structure of each ketone for both sides of attack and their relative ZPE corrected energy (E_{rel}). By using these relative energies[48] of transition state for both sides of the hydride attack, the ratios of transition states were calculated as the diastereomeric product ratio assuming the Boltzmann distribution at 25 °C (summarized in Table 2). It is seen that calculated diastereoselectivities sufficiently reproduce the tendency of the experimental diastereomeric ratios: the reduction of 4-methylcyclohexanone (**1**) gives predominant axial attack product and the reduction of 2-*tert*-butylcyclohexanone (**2**) dose not show noticeable diastereoselectivity.[49] The reliability of our proposed transition state structure is thus proved again and the utility of the present method to predict π-facial diastereoselectivity is shown. One can determine the diastereomeric product ratio of $NaBH_4$ reduction with other prochiral ketones using the same calculation based on this transition state structure. Also our previously developed EFOE model[2c] successfully reproduced these tendencies of π-facial diastereoselectivity in $NaBH_4$ reduction of substituted cyclohexanones and can explained its origin, but now further quantitative prediction of the diastereomeric product ratio can be achieved by using our new transition state structure model. In addition, more detailed investigation about the origin of this π-facial diastereoselectivity in $NaBH_4$ reduction is now feasible, and will be reported in the near future.

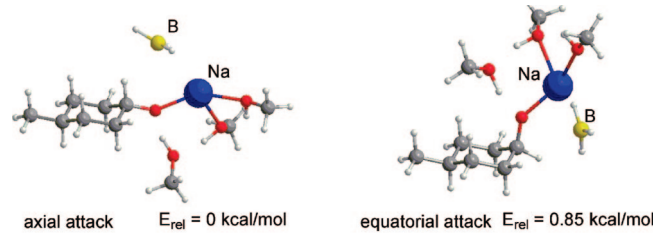

Figure 11. $NaBH_4$-4-methylcyclohexanone (**1**) transition states (MP2/6-31+G(d)//B3LYP/6-31+G(d)).

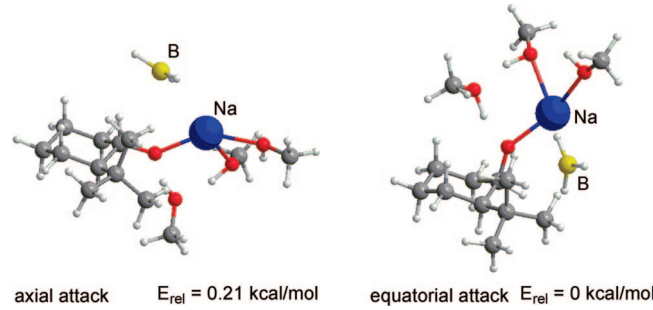

Figure 12. $NaBH_4$-2-*tert*-butylcyclohexanone (**2**) transition states (MP2/6-31+G(d)//B3LYP/6-31+G(d)).

Conclusions

Ab initio CPMD simulations have been performed to investigate the structure of $NaBH_4$ in methanol solutions as the basic study on the reaction mechanism of $NaBH_4$ reduction. By using the pointwise thermodynamic integration technique involving constrained molecular dynamics simulations, it was found that the free energy difference between associated $NaBH_4$ and dissociated Na^+ and BH_4^- in methanol solution is more than 4 kcal/mol, and it can be concluded that $NaBH_4$ is naturally associated in methanol solvent forming contact ion pairs.

According to these results, the new transition state structure model of $NaBH_4$ reduction with ketones which contains sodium cation was proposed and located by DFT optimize calculation. The catalytic effect of protic solvent is reproduced in the frame of this newly proposed transition state structure model. Calculated diastereoselectivity of the reduction of various substituted cyclohexanones using this new transition state model is in good agreement with experimental data, so its validity and effectiveness to study another system and the origin of diastereoselectivity is represented. Now we can discuss the origin of diastereoselectivity of $NaBH_4$ reduction in more detail using this transition state structure model and the entire mechanism of reaction, and this will be reported in the future.

Acknowledgment. We thank the Research Center for Computational Science, Okazaki National Research Institutes, for the use of SGI Altix4700. This work was supported by the Japan Society for the Promotion of Science (Grant No. 17550032).

Supporting Information Available: Coordinates of all transition state structures discussed in this paper. This material is available free of charge via the Internet at http://pubs.acs.org.

References and Notes

(1) Described in a series of eleven papers:Schlesinger, H. I.; Brown, H. C.; Hoekstra, H. R.; Rapp, L. R. *J. Am. Chem. Soc.* **1953**, *75*, 18–224.

(2) For recent reviews, see:(a) Gung, B. W. *Tetrahedron* **1996**, *52*, 5263–5301. (b) Dannenberg, J. J. *Chem. Rev.* **1999**, *99*, 1225–1241. (c) Tomoda, S. *Chem. Rev.* **1999**, *99*, 1243–1263. (d) Cieplak, A. S. *Chem. Rev.* **1999**, *99*, 1265–1336. (e) Ohwada, T. *Chem. Rev.* **1999**, *99*, 1337–1375. (f) Gung, B. W. *Chem. Rev.* **1999**, *99*, 1377–1385. (g) Kaselj, M.; Chung, W. S.; le Nobel, W. J. *Chem. Rev.* **1999**, *99*, 1387–1413. (h) Adcock, W.; Trout, N. A. *Chem. Rev.* **1999**, *99*, 1415–1435. (i) Mehta, G.; Chandrasekhar, J. *Chem. Rev.* **1999**, *99*, 1437–1467. (j) Wipf, P.; Jung, J.-K. *Chem. Rev.* **1999**, *99*, 1469–1480.

(3) Tomoda, S.; Senju, T. *Tetrahedron* **1997**, *53*, 9057–9066.

(4) Tomoda, S.; Senju, T. *Tetrahedron* **1999**, *55*, 3871–3882.

(5) Tomoda, S.; Senju, T. *Tetrahedron* **1999**, *55*, 5303–5318.

(6) Tomoda, S.; Senju, T. *Chem. Commun.* **1999**, 423–424.

(7) Tomoda, S.; Senju, T. *Chem. Commun.* **1999**, 621–622.

(8) Tomoda, S.; Senju, T.; Kawamura, M.; Ikeda, T. *J. Org. Chem.* **1999**, *64*, 5396–5400.

(9) Luibrand, R. T.; Taigounov, I. R.; Taigounov, A. A. *J. Org. Chem.* **2001**, *66*, 7254–7262.

(10) Bocca, C. C.; Gauze, G. F.; Basso, E. A. *Chem. Phys. Lett.* **2005**, *413*, 434–439.

(11) Bikiel, D. E.; Salvo, F. D.; Lebrero, M. C. G.; Doctorovich, F.; Estrin, D. A. *Inorg. Chem.* **2005**, *44*, 5286–5292.

(12) Suzuki, Y.; Kaneno, D.; Tomoda, S. *Tetrahedron Lett.* **2008**, *49*, 4223–4226.

(13) Wu, Y.-D.; Tucker, J. A.; Houk, K. N. *J. Am. Chem. Soc.* **1991**, *113*, 5018.

(14) Yadav, V. K.; Jeyaraj, D. A.; Balamurugan, R. *Tetrahedron* **2000**, *56*, 7581–7589.

(15) Wigfield, D. C.; Gowland, F. W. *Tetrahedron Lett.* **1976**, *17*, 3373–3376.

(16) Wigfield, D. C.; Gowland, F. W. *J. Org. Chem.* **1977**, *42*, 1108–1109.

(17) Wigfield, D. C. *Tetrahedron* **1979**, *35*, 449–462.

(18) Dewer, M. J. S.; McKee, M. L. *J. Am. Chem. Soc.* **1978**, *100*, 7499–7505.

(19) Eisenstein, O.; Schlegel, H. B.; Kayser, M. M. *J. Org. Chem.* **1982**, *47*, 2886–2891.

(20) Yamataka, H.; Terukiyo, H. *J. Am. Chem. Soc.* **1986**, *108*, 6643–6646.

(21) Gatling, S. C.; Jackson, J. E. *J. Am. Chem. Soc.* **1999**, *121*, 8655–8656.

(22) Han, W. H.; Li, H. R.; Deng, D. S.; Wang, Y. *Acta Chim. Sin.* **2006**, *64*, 1723–1729.

(23) Glass, R. S.; Deardorff, D. R.; Henegar, K *Tetrahedron Lett.* **1980**, *21*, 2467–2470.

(24) Car, R.; Parrinello, M. *Phys. Rev. Lett.* **1985**, *55*, 2471–2474.

(25) Tse, J. S. *Annu. Rev. Phys. Chem.* **2002**, *53*, 249–290.

(26) There have been so many successful results with CPMD simulation to deal with the solutes and solvents dynamics. See the publication list on the CPMD consortium page (http://www.cpmd.org/cpmd_publications.html).

(27) Sprik, M.; Ciccotti, G. *J. Chem. Phys.* **1998**, *109*, 7737–7744, and references cited therein.

(28) *CPMD*, version 3.13.1; http://www.cpmd.org/; Copyright IBM Corp 1990−2008, Copyright MPI für Festkörperforschung Stuttgart 1997−2001.

(29) Troullier, N.; Martins, J. L. *Phys. Rev. B* **1991**, *43*, 1993–2006.

(30) Kleinman, L.; Bylander, D. M. *Phys. Rev. Lett.* **1982**, *48*, 1425–1428.

(31) Vuilleumier, R.; Sprik, M. *J. Chem. Phys.* **2001**, *115* (8), 3454–3468.

(32) Pagliai, M.; Cardini, G.; Righini, R.; Schettino, V. *J. Chem. Phys.* **2003**, *119*, 6655–6662.

(33) Goedecker, S.; Teter, M.; Hutter, J. *Phys. Rev. B* **1996**, *54*, 1703–1710.

(34) Faralli, C.; Pagliai, M.; Cardini, G.; Schettino, V. *Theor. Chem. Acc.* **2007**, *118*, 417–423.

(35) Pagliai, M.; Cardini, G.; Schettino, V. *J. Phys. Chem. B* **2005**, *109*, 7475–7481.

(36) Faralli, C.; Pagliai, M.; Cardini, G.; Schettino, V. *J. Phys. Chem. B* **2006**, *110*, 14923–14928.

(37) Faralli, C.; Pagliai, M.; Cardini, G.; Schettino, V. *J. Chem. Theory Comput.* **2008**, *4*, 156–163.

(38) Becke, A. D. *Phys. Rev. A* **1988**, *38*, 3098–3100.

(39) Lee, C.; Yang, W.; Parr, R. G. *Phys. Rev. B* **1988**, *37*, 785–789.

(40) Frisch, M. J.; Trucks, G. W.; Schelegel, H. B.; Scuseria, G. E.; Robb, M. A.; Cheeseman, J. R.; Montgomery, Jr., J. A.; Vreven, T.; Kudin, K. N.; Burant, J. C.; Millam, J. M.; Iyengar. S. S.; Tomasi, J.; Barone, V.; Mennucci, B.; Cossi, M.; Scalmani, G.; Rega, N.; Petersson, G. A.; Nakatsuji, H.; Hada, M.; Ehara, M.; Toyota, K.; Fukuda, R.; Hasegawa, J.; Ishida, M.; Nakajima, T.; Honda, Y.; Kitao, O.; Nakai, H.; Klene, M.; Li, X.; Knox, J. E.; Hratchian, H. P.; Cross, J. B.; Bakken, V.; Adamo, C.; Jaramillo, J.; Gomperts, R.; Stratmann, R. E.; Yazyev, O.; Austin, A. J.; Cammi, R.; Pomelli, C.; Ochterski, J. W.; Ayala, P. Y.; Morokuma, K.; Voth, G. A.; Salvador, P.; Dannenberg, J. J.; Zakrzewski, V. G.; Dapprich, S.; Daniels, A. D.; Strain, M. C.; Farkas, O.; Malick, D. K.; Rabuck, A. D.; Raghavachari, K.; Foresman, J. B.; Ortiz, J. V.; Cui, Q.; Baboul, A. G.; Clifford, S.; Cioslowski, J.; Stefanov, B. B.; Liu, G.; Liashenko, A.; Piskorz, P.; Komaromi, I.; Martin, R. L.; Fox, D. J.; Keith, T.; Al-Laham, M. A.; Peng, C. Y.; Nanayakkara, A.; Challacombe, M.; Gill, P. M. W.; Johnson, B.; Chen, W.; Wong, M. W.; Gonzalez, C.; Pople, J. A. *Gaussian 03*, revision D.01; Gaussian Inc.: Wallingford, CT, 2004.

(41) Becke, A. D. *J. Chem. Phys.* **1993**, *98*, 5648.

(42) Hummer, G.; Pratt, L. R.; García, A. E. *J. Phys. Chem. A* **1998**, *102*, 7885–7895.

(43) Suzuki, Y.; Kaneno, D.; Tomoda, S. Unpublished data.

(44) Hammond, G. S. *J. Am. Chem. Soc.* **1955**, *77*, 334.

(45) The effect of higher solvation shells is often estimated by a continuum model. The value of the activation energy of the reduction of acetone obtained by using conductor polarizable continuum model (CPCM) calculation is 12.0 kcal mol^{-1}, which is also in agreement with experiment.

(46) Wigfield, D. C.; Phelps, D. J. *J. Org. Chem.* **1976**, *41*, 2396–2401.

(47) Wigfield, D. C.; Phelps, D. J. *J. Am. Chem. Soc.* **1974**, *96*, 543–549.

(48) It should be noted that the energy difference between the diastereomeres is small, less than 1 kcal/mol, which is within the accuracy of the DFT method using the 6-31+G(d) basis.

(49) The result of the case with the CPCM continuum solvation model to estimate the effect of higher solvation shells is the following: in the reduction of 4-methylcyclohexanone the axial attack is predominant by 0.88 kcal mol^{-1}, and in the reduction of 2-*tert*-butylcyclohexanone the equatorial attack is predominant by 0.12 kcal mol^{-1}. These results are almost the same as the result of the case in which the effect of higher solvation shells is not considered, showing it should not affect our result significantly.

JP809966U